Stochastic Geometry-Based MCS Adaption Analysis for Uplink Cellular Networks

Xinyi Guo*§, Qiong Liu†‡, Shanshan Wang†‡, and Li You*§
*National Mobile Communications Research Laboratory, Southeast University, Nanjing 210096, China
§Purple Mountain Laboratories, Nanjing 211100, China
†LTCI, Télécom Paris, Institut Polytechnique de Paris, 91120, Palaiseau, France
‡ETIS UMR 8051, CYU, ENSEA, CNRS, 95000, Cergy, France
Email: {xinyiguo, lyou}@seu.edu.cn, qiong.liu@ensea.fr, shanshan.wang@telecom-paris.fr

***Abstract*—The link adaptation plays a crucial role in the fifth generation (5G) and future wireless networks, where adaptive modulation and coding (AMC) is vital for significantly increasing the data transmission rate and quality of service (QoS) by adjusting the modulation and coding scheme (MCS). In this work, we investigate the stochastic geometry-based MCS adaption for the uplink cellular networks with Poisson distributed base stations (BS) and user equipments (UE). We first define the conditional received rate by quantizing the channel quality, i.e., signal to interference ratio (SIR), using the sets of thresholds. Basically, higher SIR indicates better channel condition and applys higher order of modulation scheme, which leads to higher received rate. We then derive the framework of meta distribution on the conditional received rate, the spatially-average spectral efficiency (SE), and the variance of the SE. In addition, beta approximation and several bounds are presented to simplify the calculation of meta distribution. We validate the proposed framework by numerical simulations under different system parameters.**

I. Introduction

The fifth generation (5G) and beyond wireless networks are designed to support wider range of services, from ultra-reliable Internet of Things (IoT) applications to high-bandwidth multimedia services [1]. Such networks will deliver high reliability, extensive connectivity, and low latency while managing limited resources and transmission power. A key strategy in meeting these demands is adaptive modulation and coding (AMC), which dynamically adjusts modulation and coding schemes (MCS) based on the channel conditions, thereby significantly enhancing data transmission rates and quality of service (QoS) [2].

Traditionally, AMC issues have been extensively studied in the cases of a single cell or a finite number of cells [3], with MCS decisions based on the Shannon channel capacity in narrow-band fading channels. Recent developments in MCS have integrated technologies like massive multiple-input multiple-output (MIMO) and non-orthogonal multiple access (NOMA) [4] for emerging requirements. Concurrently, methodologies like machine learning algorithms have been extensively studied to enhance link adaption [5] and MCS prediction [6]. However, these methodologies often assume a fixed set of transmitters and receivers and do not account for the stochastic nature of their distributions. This randomness leads to significant variability in interference originating from stochastic locations of nodes.

Additionally, spatial stochastic modeling of wireless networks for performance analysis has become a topic of interest [7]. Stochastic geometry (SG) provides a mathematical framework to analyze the performance of large-scale wireless networks by capturing the inherent randomness in the wireless communication, including fading, shadowing and node distribution, etc [7], [8]. SG also shows its potential in evaluating the performance of wireless networks in different scenarios, e.g., millimeter Wave (mmWave) and Terahertz (THz) communication [7], cell-free massive MIMO networks [9], reconfigurable intelligent surface (RIS)-assisted networks [10], etc.

Despite fruitful studies focusing on modeling the new features in wireless networks, few references explore the integration of MCS adaptation, which is beyond the signal to interference plus noise ratio (SINR) or coverage analysis. In [8], an analytical framework is presented to assess service block probability in the downlink networks, where the services are classified according to MCS adaptation. Similarly, [11] analyzes the spectral efficiency (SE) and binary rate (BR) in uplink networks with interference-aware muting, based on MCS from the long-term evolution (LTE) standard. However, these studies predominantly focus on the average user performance in the whole network, potentially overlooking detailed insights into individual user experiences, such as the variation experienced by a single user. To address this limitation, we adopt the meta distribution [12], [13], which facilitates a fine-grain analysis of performance metrics by incorporating higher-order moments of the conditional received rate.

In this paper, we investigate the impact of MCS in the uplink networks with Poisson distributed base stations (BS) and user equipments (UE). The conditional received rate is defined by quantizing the quality of the received signal, i.e., signal to interference ratio (SIR), using predefined thresholds. A higher SIR enables a higher-order modulation scheme, increasing the data rate. The main contributions are as follows:

- *SG-based MCS modeling in the uplink*. This work

This work was supported by the National Natural Science Foundation of China for Outstanding Young Scholars under Grant 62322104, the Jiangsu Province Major Science and Technology Project under Grant BG2024005, the Natural Science Foundation of Jiangsu Province under Grant BK20231415, and the Fundamental Research Funds for the Central Universities under Grant 2242022k60007.

presents a detailed framework combining MCS and SG for uplink modeling. We introduce the meta distribution to provide a more comprehensive network performance analysis, offering insights into conditional received rates, spatially-average SE, and their variance under AMC schemes.
- *Practical considerations in uplink modeling*. Various practical aspects are considered, including uplink power control [7] and the approximated modeling of interfering UEs [14]. We analyze the system performance across different parameter settings, such as power control coefficients and UE activity factors, further demonstrating their impact on the performance evaluation.

The rest of the paper is organized as follows. Section II presents the system model and the assumptions. The main performance analysis is established in Section III. Section IV provides the simulation results, and conclusions are drawn in Section V.

II. System Model

A. Network Topology

A single-tier uplink cellular network is considered whose BSs lie in $\mathbb{R}^2$ following an independent and homogeneous Poisson point process (PPP) Φ_{BS}, with intensity λ_{BS}. The UE are spatially distributed following homogeneous PPP Φ_{UE} with intensity λ_{UE}. Here in the current paper, we assume that UE density is much higher than BS density, i.e., $\lambda_{\text{UE}} >> \lambda_{\text{BS}}$, such that each BS has at least one UE associated with it in one resource block. Moreover, each UE is associated with its closest BS, thereby forming a Voronoi cell tessellation [7]. The selected UE point process is modeled as $\Phi_u \triangleq \{U(V(y))|y \in \Phi_{\text{BS}}\}$, where $V(y)$ denotes the Voronoi cell of the BS $y \in \Phi_{\text{BS}}$, and $U(V(y))$ denotes an arbitrary point chosen within $V(y)$. The typical BS is located at the origin for the simplicity of analysis, with its associated UE located at x_0. We denote the interfering UE point process as Φ_{I}, given by $\Phi_{\text{I}} = \Phi_u \setminus \{x_0\}$.

B. Signal-to-Interference Ratio

In an interference-limited scenario, we focus on the three types of distances between BSs and UEs. The distance between typical BS at the origin o, i.e., BS_o, and its associated UE $x_0 \in \Phi_u$ is denoted as R. The distance between typical BS_o and the interfering UE $x \in \Phi_{\text{I}}$ is denoted by D_x. Additionally, we denote the distance between the interfering UE $x \in \Phi_{\text{I}}$ and its associated BS as R_x. We assume that the BS and each UE are equipped with a single antenna.

To partially compensate for path loss, we introduce the fractional power control (FPC) scheme [12] at each UE $x \in \Phi_u$, given by $P_x = p_0 R_x^{\eta\epsilon}$, where $\epsilon \in [0, 1]$ is the power control coefficient, and η stands for the path loss exponent. For example, the FPC at UE x_0 is $P_{x_0} = p_0 R^{\eta\epsilon}$. Note that when $\epsilon = 0$, no power control is applied at the UE, and when $\epsilon = 1$ corresponds to full path-loss inversion power control. Thus, the received SIR γ experienced at the typical BS is

$$\gamma = \frac{P_{x_0} H_{x_0} R^{-\eta}}{\sum_{x \in \Phi_{\text{I}}} P_x \beta_x H_x D_x^{-\eta}}, \tag{1}$$

where H_x and H_{x_0} are the channel gains between the typical BS and the interfering UE at position x and its associated UE at position x_0, respectively, which are assumed to be exponentially distributed. β_x represents the activity factor of the UE located at x, which follows Bernoulli distribution with parameter q. Note that β_x can be seen as the probability that one UE is active or the fraction of active interfering UEs due to the independent activation from each UE.

C. Link Distance Distributions on R and R_x

In uplink cellular networks, the interfering UEs, i.e., Φ_{I}, form a non-stationary process, due to the Poisson-Voronoi tessellation among cells [14]. Therefore, as in [12], we approximate the interference distribution Φ_{I} at BS_o as inhomogeneous PPP, with intensity function as following

$$\lambda_{\text{I}}(x) = \lambda_{\text{BS}}(1 - e^{-B_2 \lambda_{\text{BS}} \pi D_x^2}), \tag{2}$$

the probability density function (PDF) of the distance R between BS_o and UE x_0, $f_R(r)$, is given by

$$f_R(r) = 2B_1 \pi \lambda_{\text{BS}} r e^{-2B_1 \lambda_{\text{BS}} \pi r^2}, r \geq 0, \tag{3}$$

where $B_1 = \frac{5}{4}$, $B_2 = \frac{12}{5}$.

The distribution of the distance R_x follows the same statistical law as R since all cells are assumed to be statistically homogeneous. However, R_x is constrained by the distance D_x (i.e., $R_x \leq D_x$). Therefore, the distribution of R_x, conditioned on D_x, is described as the truncated Rayleigh distribution [12]

$$f_{R_x}(r|D_x) = \frac{2B_1 \pi \lambda r e^{-B_1 \lambda \pi r^2}}{1 - e^{-B_1 \lambda \pi D_x^2}}, 0 \leq r \leq D_x. \tag{4}$$

The conditional distribution in (4) reflects the statistical dependency imposed by the spatial structure of the network and ensures that R_x remains within the distance D_x.

Remark 1: It should be noted that D_x does not necessarily have to be greater than R. But D_x must be no less than R_x. It indicates that an interfering UE x from a neighboring cell can be much closer to BS_o than the UE x_o. The latter is due to the smallest distance association between selected UE and receiving BS.

D. MCS Adaption

In cellular networks, traffic is scheduled using multiple MCSs, where each MCS is associated with a specific SIR threshold [15]. The SIR depends on the UE location and fading, making the received rate at a typical BS location-dependent. In the uplink network, AMC works by UEs transmitting sounding reference signals for BSs to estimate SIR. Based on these estimations, BSs select the MCS, which is linked to a channel quality indicator (CQI), thus optimizing SE while maintaining the block error rate (BLER). Actually, incorporating multiple MCSs in scheduling can significantly improve SE.

We conceptualize the MCS as follows: The condition of the channel is categorized into M distinct, non-overlapping intervals. Each interval corresponds to a specific state linked to an MCS strategy. We define $\Theta = \{\theta_1, \theta_2, \ldots, \theta_M\}$ as a set of SIR thresholds, where $\theta_1 < \cdots < \theta_M$ and $\theta_i \in \mathbb{R}^+$. These thresholds segment the continuous SIR into $M+1$ discrete zones, denoted as $i_{\text{CQI}} \in \{0, 1, 2, \ldots, M\}$. Here, a channel state i_{CQI} is considered better to j_{CQI} for all $i > j$, and $\cap_{i_{\text{CQI}}=0}^{M} [\theta_{i_{\text{CQI}}}, \theta_{i_{\text{CQI}+1}}] = \emptyset$, where we set $\theta_0 = -\infty$ and $\theta_{M+1} = +\infty$ as a complement. Consequently, the proportion of SIR that falls within the i_{CQI}-th region equals the probability $\mathbb{P}(\theta_{i_{\text{CQI}}} < \gamma < \theta_{i_{\text{CQI}}+1})$. For a typical link, we define the received rate for each MCS region by the corresponding SIR

$$R_{\text{MCS}}(\gamma) = r_{i_{\text{CQI}}} \mathbb{1}(\theta_{i_{\text{CQI}}} \leq \gamma < \theta_{i_{\text{CQI}+1}}), \tag{5}$$

where $\mathbb{1}(.)$ denotes the indicator function, $r_{i_{\text{CQI}}}$ is the rate corresponding to the SIR level and indexed by i_{CQI}. Note that $r_1 < r_2 < \cdots < r_M$ and $r_0 = 0$. This setup reflects the fact that higher SIR values allow for the use of higher-order MCS, thus leading to higher received rates.

III. Performance Analysis

In this section, we analyze uplink cellular network performance by first presenting the expression of the conditional received rate, followed by the analysis of its meta distribution including the exact expression, beta approximation and classical bounds. Finally, we discuss the spatially-average SE of the network and the variance of the SE.

A. Conditional Received Rate

For a given UE x_0 associated with the BS_o, and given a realization of Φ_u and Φ_{BS}, the expectation of the conditional received rate with MCS is denoted as

$$\begin{aligned} r(\Phi_{\text{BS}}, \Phi_u) &= \mathbb{E}\left[R_{\text{MCS}}(\gamma) \middle| \Phi_{\text{BS}}, \Phi_u\right] \\ &= \mathbb{E}\left[r_{i_{\text{CQI}}} \mathbb{1}(\theta_{i_{\text{CQI}}} \leq \gamma < \theta_{i_{\text{CQI}+1}}) | \Phi_{\text{BS}}, \Phi_u\right]. \end{aligned} \tag{6}$$

By calculating the expectation over the channel fading and the activity factor of interfering UEs, we can further simplify the expression of the conditional received rate.

Lemma 1 (Conditional received rate): The conditional received rate experienced by the typical BS is

$$r(\Phi_{\text{BS}}, \Phi_u) = \sum_{m=1}^{M} \Delta r_m \prod_{x \in \Phi_{\text{I}}} f(\theta_m), \tag{7}$$

where $\Delta r_m = r_m - r_{m-1}$ and $f(\theta_m) = \frac{q}{1+\theta_m R^{\eta(1-\epsilon)} R_x^{\eta\epsilon} D_x^{-\eta}} + 1 - q$.

Proof 1: See Appendix A.

Lemma 1 presents the conditional data rate from a given UE, conditioned on a specific realization of the network. It captures the randomness of BS locations, UE locations, and channel fading on the received data rate.

B. Meta Distribution

The meta distribution characterizes user-specific behavior across different spatial realizations of the network, providing information on the fraction of UEs that achieve a rate above a given threshold.

Definition 1 (Meta distribution of conditional received rate): Given the SIR thresholds Θ for the MCS region and the data rate threshold ξ, the meta distribution of conditional received rate is defined as:

$$\bar{F}(\Theta, \xi) = \mathbb{P}\left(r(\Phi_{\text{BS}}, \Phi_u) > \xi\right), \tag{8}$$

where $\Theta = \{\theta_1, \ldots, \theta_M\}$ is the set of SIR thresholds as detailed in Section II-D, and $\xi \in \mathbb{R}^+$.

For example, if $\bar{F} = 0.9$ and $\xi = 2$ Gbps, the probability that the conditional received rate exceeds 2 Gbps is 90%, i.e., 90% of the typical links can achieve the data rate above 2 Gbps.

1) Moments: According to the definition in [12], the b-th moment of the conditional received rate is given by

$$\begin{aligned} M_b &= \mathbb{E}\left[r(\Phi_{\text{BS}}, \Phi_u)^b\right] \\ &= \mathbb{E}\left[\left(\sum_{m=1}^{M} \Delta r_m \prod_{x \in \Phi_{\text{I}}} f\left(\theta_m\right)\right)^b\right], \end{aligned} \tag{9}$$

where $b \in \mathbb{N}^+$.

Theorem 1 (General cases for moments): The b-th moment of the conditional received rate is given by

$$M_b = \sum_{\substack{n_1, n_2 \cdots, n_M \geq 0 \\ n_1 + n_2 + \cdots + n_M = b}} \frac{b!}{n_1! n_2! \cdots n_M!} (\prod_{m=1}^{M} \Delta r_m^{n_m}) g(\theta_m), \tag{10}$$

where

$$g(\theta_m) = \int_0^\infty e^{-z\left(1+\int_0^\infty f(x,z,\theta_m)\mathrm{d}x\right)} \mathrm{d}z, \tag{11}$$

and

$$\begin{aligned} f(x,z,\theta_m) = &\int_0^x \frac{z e^{-zy}\left(1 - e^{\frac{B_2}{B_1} zx}\right)}{B_1\left(1 - e^{-zx}\right)} \\ &\left(1 - \prod_{m=1}^{M}\left(1 - \frac{q\theta_m}{\theta_m + y^{-\frac{\eta\epsilon}{2}} x^{\frac{\eta}{2}}}\right)^{n_m}\right) \mathrm{d}y. \end{aligned} \tag{12}$$

Proof 2: See Appendix B.

Definition 2 (SE): The SE of the typical link based on the received SIR γ is defined as follows [11]

$$\text{SE}_{\text{MCS}} = \sum_{i_{\text{CQI}}=0}^{M} \text{SE}_{i_{\text{CQI}}} \mathbb{1}\left(\gamma \in \left[\theta_{i_{\text{CQI}}}, \theta_{i_{\text{CQI}}+1}\right)\right), \tag{13}$$

where $\text{SE}_{i_{\text{CQI}}}$ represents the SE corresponding to the MCS region indexed by i_{CQI}.

Under our system settings, the spatially-average SE is exactly the first moment M_1 normalized by bandwidth. The variance of SE is given by $M_2 - M_1^2$, where M_b is given in Theorem 1.

Lemma 2 (Spatially-average SE): The spatially-average of SE is given by

$$\mathrm{SE}(\Theta)=\mathbb{E}[\mathrm{SE}_{\mathrm{MCS}}]=\sum_{m=1}^{M}\Delta s_m\int_0^{\infty}e^{-z\left(1+\int_0^{\infty}f(x,z,\theta_m)\mathrm{d}x\right)}\mathrm{d}z. \tag{14}$$

where $\Delta s_m = \mathrm{SE}_m - \mathrm{SE}_{m-1}$ and

$$f(x,z,\theta_m)=\int_0^x \frac{ze^{-zy}\left(1-e^{-\frac{B_2}{B_1}zx}\right)q\theta_m}{B_1\left(1-e^{-zx}\right)\left(\theta_m+y^{-\frac{\eta\epsilon}{2}}x^{\frac{\eta}{2}}\right)}\mathrm{d}y. \tag{15}$$

Lemma 3 (Variance of SE): The variance of SE is given by

$$\mathrm{Var}[\mathrm{SE}_{\mathrm{MCS}}]=\sum_{m=1}^{M}\sum_{n=1}^{M}\Delta s_m\cdot\Delta s_n \int_0^{\infty}e^{-z\left(1+\int_0^{\infty}f_1(x,z,\theta_m,\theta_n)\mathrm{d}x\right)}\mathrm{d}z-\mathrm{SE}(\Theta)^2, \tag{16}$$

where $\Delta s_m = \mathrm{SE}_m - \mathrm{SE}_{m-1}$, $\mathrm{SE}(\Theta)$ follows from Lemma 2 and

$$f_1(x,z,\theta_m,\theta_n)=\int_0^x \frac{ze^{-zy}\left(1-e^{-\frac{B_2}{B_1}zx}\right)}{B_1\left(1-e^{-zx}\right)}\Bigg(\frac{q\theta_m}{\theta_m+x^{\frac{\eta}{2}}y^{-\frac{\eta\epsilon}{2}}} +\frac{q\theta_n}{\theta_n+x^{\frac{\eta}{2}}y^{-\frac{\eta\epsilon}{2}}}-\frac{q^2\theta_m\theta_n}{\left(\theta_m+x^{\frac{\eta}{2}}y^{-\frac{\eta\epsilon}{2}}\right)\left(\theta_n+x^{\frac{\eta}{2}}y^{-\frac{\eta\epsilon}{2}}\right)}\Bigg)\mathrm{d}y. \tag{17}$$

Lemma 2 presents the spatially-average SE, which is the summation of the functions related to the m-th CQI region; Lemma 3 highlights SE fluctuations between links, with higher variance indicating greater disparity and reduced UE fairness.

Corollary 1 (Equally partition): When $M=2$, i.e., the SIR region is equally divided into two, we have $\Delta f=\Delta r_2=\Delta r_1$ and

$$M_b=\Delta f^b\sum_{k=0}^{\infty}\frac{\Gamma(b+1)}{\Gamma(k+1)\Gamma(b-k+1)}g(\theta_1,\theta_2), \tag{18}$$

where

$$g(\theta_1,\theta_2)=\int_0^{\infty}e^{-z\left(1+\int_0^{\infty}f(x,z,\theta_1,\theta_2)\mathrm{d}x\right)}\mathrm{d}z, \tag{19}$$

and

$$f(x,z,\theta_1,\theta_2)=\int_0^x \frac{ze^{-zy}\left(1-e^{-\frac{B_2}{B_1}zx}\right)}{B_1\left(1-e^{-zx}\right)}\Bigg(1-\left(1-\frac{q\theta_1}{\theta_1+y^{-\frac{\eta\epsilon}{2}}x^{\frac{\eta}{2}}}\right)^k\left(1-\frac{q\theta_2}{\theta_2+y^{-\frac{\eta\epsilon}{2}}x^{\frac{\eta}{2}}}\right)^{b-k}\Bigg)\mathrm{d}y. \tag{20}$$

2) Exact Expression of Meta Distribution: Using the Gil-Pelaez inversion theorem [12], an exact integral expression of meta distribution can be obtained from the purely imaginary moments $\varphi(iw)$, where $i\triangleq\sqrt{-1}$.

Theorem 2 (Exact expression): The meta distribution of the conditional received rate is given by

$$\bar{F}(\Theta,\xi)=\frac{1}{2}+\frac{1}{\pi}\int_0^{\infty}\frac{1}{w}\mathrm{Im}\left\{u^{-iw}\varphi\left(iw\right)\right\}dw, \tag{21}$$

where $\varphi(iw)=M_{iw}$ and M_{iw} are defined in (9), and $\mathrm{Im}\{\cdot\}$ represents the imaginary part of a complex number.

3) Beta Approximation: The calculation of the exact integral expression for meta distribution takes a long time to converge. This is because the $\binom{iw}{k}$ is subject to oscillatory convergence, which converges more slowly as w increases. Given that $\tilde{r}(\Phi_{\mathrm{BS}},\Phi_u)=\frac{r(\Phi_{\mathrm{BS}},\Phi_u)}{r_M}$ is supported on [0,1], a natural choice for a simple approximation is the beta distribution [12]. The PDF of the beta distribution is $f(x;\alpha,\beta)=\frac{1}{B(\alpha,\beta)}x^{\alpha-1}(1-x)^{\beta-1}$, where beta function $B(\alpha,\beta)=\frac{\Gamma(\alpha)\Gamma(\beta)}{\Gamma(\alpha+\beta)}$, and α and β are shape parameters. The expectation and variance of beta distributed random variable X are as follows, respectively

$$\mu=\mathbb{E}[X]=\frac{\alpha}{\alpha+\beta}, \tag{22}$$

$$\mathrm{Var}[X]=\mathbb{E}[X-\mu]^2=\frac{\alpha\beta}{(\alpha+\beta)^2(\alpha+\beta+1)}. \tag{23}$$

Hence, we can approximate the meta distribution in (21) by fitting $M_1(M_1=\mu)$ and $M_2\left(M_2=\mathrm{Var}\left[X\right]+M_1^2\right)$ into the corresponding moments of beta distribution. Then the shape parameters α and β can be written as

$$\beta=\frac{(1-M_1)(M_1-M_2)}{M_2-M_1^2}, \tag{24}$$

$$\alpha=\frac{\beta M_1}{1-M_1}=\frac{M_1(M_1-M_2)}{M_2-M_1^2}. \tag{25}$$

With the help of beta approximation, we are able to approximate the distribution of $\tilde{r}(\Phi_{\mathrm{BS}},\Phi_u)$ and $r(\Phi_{\mathrm{BS}},\Phi_u)$.

4) Classical Bounds: The lower and upper boundary of meta distribution can be obtained by applying Markov and Chebyshev bounds as in [12]. Noting that for $\xi>r_M$, we have $\bar{F}(\Theta,\xi)=0$, our discussion is focused on the region $\xi\in[0,r_M]$. For $b>0$, the Markov bounds for meta distribution of $r\left(\Phi_{\mathrm{BS}},\Phi_u\right)$ are

$$1-\frac{\mathbb{E}\left[\left(r_M-r\left(\Phi_{\mathrm{BS}},\Phi_u\right)\right)^b\right]}{(r_M-\xi)^b}<\bar{F}(\Theta,\xi)\leq\frac{M_b}{\xi^b}. \tag{26}$$

Unlike the Markov inequality, the Chebyshev inequality accounts for the variance of the random variable. Since we have $\xi\in[0,r_M]$ and $M_1\in[0,r_M]$, the relationship between ξ and M_1 must be analyzed case by case. The Chebyshev bounds are given as follows. For $\xi<M_1$,

$$\bar{F}(\Theta,\xi)>1-\frac{V}{(\xi-M_1)^2},\ \forall\xi<M_1, \tag{27}$$

while for $\xi>M_1$,

$$\bar{F}(\Theta,\xi)\leq\frac{V}{(\xi-M_1)^2},\ \forall\xi\geq M_1, \tag{28}$$

where $V\triangleq\mathrm{Var}\left[r(\Phi_{\mathrm{BS}},\Phi_u)\right]=M_2-M_1^2$.

IV. Numerical Results

In this section, we validate the SE, beta approximation, as well as the bounds mentioned in Section III by Monte-Carlo simulations. The impact of system parameters, e.g., activity factor q, power control coefficient ϵ, is further analyzed. In the simulation settings, we consider BS density $\lambda_{\mathrm{BS}}=0.25$, path loss exponent $\eta=4$.

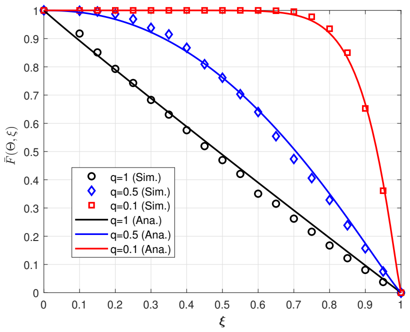

Fig. 1. The meta distribution with $\Delta f = 0.5$ under different activity factor q.

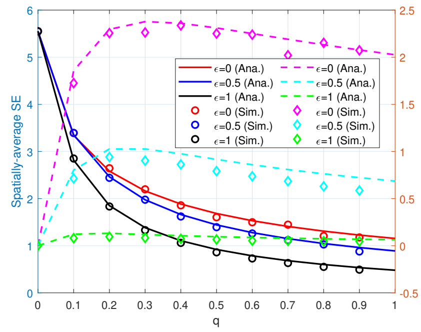

Fig. 2. Spatially-average SE and the variance of SE.

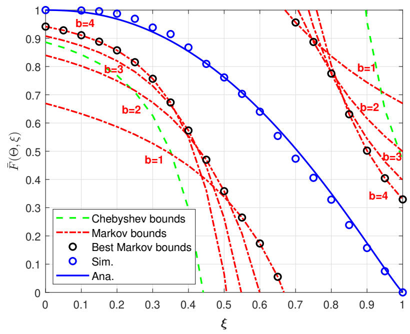

Fig. 3. The analytical bounds and simulation results on meta distribution.

Fig. 1 illustrates the results from Theorem 2, showing the performance of UE-BS links under various normalized data rate thresholds ξ and UE activity factors q, based on the scenario outlined in Corollary 1. Here, the SIR region is divided equally with parameters $\Delta f = 0.5$, $\theta_1 = 0$ dB, and $\theta_2 = 5$ dB. Each UE's power control coefficient is set at $\epsilon = 0.5$. For instance, at $\xi = 0.4$ and $q = 1$, 60% of links achieve the threshold, indicating the proportion of UE-BS links that meet or exceed ξ. The beta distribution accurately approximates the meta distribution of the received rate, with simulations aligning well with analytical predictions. Additionally, with a constant UE activity factor q, the meta distribution declines as ξ increases, indicating that fewer links surpass higher rate thresholds. Furthermore, an increase in q, corresponding to more active interfering UEs, reduces the likelihood that the typical link's received rate will exceed ξ, due to heightened interference.

Fig. 2 illustrates the spatially-average SE (left axis) in Lemma 2 and the variance of SE (right axis) in Lemma 3 versus activity factor q under various power control coefficients ϵ. The SIR threshold and SE values are taken from the link simulator as detailed in [11]. We observe that the spatially-average SE decreases with the increase of q when ϵ is fixed. This is due to the increase in the number of interferers, which deteriorates the SIR and consequently lowers the SE. Taking both the spatially-average SE and the variance of SE into consideration, we conclude that the variance of SE decreases dramatically with the help of FPC, while the spatially-average SE has only slightly decreased.

Fig. 3 presents the classical bounds for the meta distribution, comparing the simulation results, Chebyshev bounds, Markov bounds, and the best Markov bounds across different values of the moment parameter b ranging from 1 to 4. The graph indicates that Markov bounds (dashed red lines) generally offer tighter estimates than Chebyshev bounds (dashed green lines), especially for higher b values. For the lower bounds, as ξ decreases, Markov bounds with larger b become closer to the simulation values, while for the upper bounds, larger b values provide tighter bounds at higher ξ. Overall, these bounds offer a quick way to assess network performance.

V. Conclusion

In this paper, we presented a framework for analyzing the impact of MCS in uplink cellular networks. Considering Poisson distributed BSs and UEs, we defined the conditional received rate by quantizing the channel quality and applying the matching modulation scheme. Using SG, we derived the meta distribution of the conditional received rate, spatially-average SE and the variance of the SE. Additionally, we applied the beta approximation and several classical bounds for faster calculation of the meta distribution. The numerical results validated the above analytical results under different system parameters.

Appendix

A. Proof of Lemma 1

Given the received rate at each MCS region, the conditional received rate of the typical link is

$$r(\Phi_{\rm BS},\Phi_u)=\mathbb{E}[R_{\rm MCS}(r)|\Phi_{\rm BS},\Phi_u] \overset{(a)}{=} \sum_{m=0}^{M} r_m \mathbb{P}(\theta_m<\gamma<\theta_{m+1})$$
$$\overset{(b)}{=} \sum_{m=1}^{M} \Delta r_m \mathbb{P}\left(\frac{H_{x_0}R^{\eta(\epsilon-1)}}{\sum_{x\in\Phi_{\rm I}}\beta_x H_x R_x^{\eta\epsilon} D_x^{-\eta}} > \theta_m|\Phi_{\rm BS},\Phi_u\right), \quad (29)$$

where (a) follows from (5), (b) follows from (1) and the FPC. Given that $H_x \sim \exp(1)$ and $\beta_x \sim B(1,q)$, part of the (29) can by simplified as

$$\mathbb{P}\left(\frac{H_{x_0}R^{\eta(\epsilon-1)}}{\sum_{x\in\Phi_{\rm I}}\beta_x H_x R_x^{\eta\epsilon} D_x^{-\eta}} > \theta_m|\Phi_{\rm BS},\Phi_u\right)$$
$$=\mathbb{E}_{H_x,\beta_x}\left[\prod_{x\in\Phi_{\rm I}} e^{-\theta_m R^{\eta(1-\epsilon)}\beta_x H_x R_x^{\eta\epsilon} D_x^{-\eta}}\middle|\Phi_{\rm BS},\Phi_u\right]$$
$$=\prod_{x\in\Phi_{\rm I}}\left(\frac{q}{1+\theta_m R^{\eta(1-\epsilon)}R_x^{\eta\epsilon}D_x^{-\eta}}+1-q\right). \quad (30)$$

Thus, the proof is complete.

B. Proof of Theorem 1

Considering the definition of moments, we give the b-th moments of the conditional received rate as follows

$$M_b = \mathbb{E}[r(\Phi_{\rm BS},\Phi_u)^b] \overset{(a)}{=} \mathbb{E}[\left(\sum_{m=1}^{M}\Delta r_m \prod_{x\in\Phi_{\rm I}} f(\theta_m)\right)^b]$$
$$\overset{(b)}{=} \sum_{C_1,C_2} A\left(\prod_{m=1}^{M}\Delta r_m^{n_m}\right)\mathbb{E}\left[\prod_{x\in\Phi_{\rm I}}\prod_{m=1}^{M} f(\theta_m)^{n_m}\right], \quad (31)$$

where (a) is obtained by (7) where $A = \frac{b!}{n_1! n_2! \cdot\cdot n_M!}$ and

$f(\theta_m) = \frac{q}{1+\theta_m R^{\eta(1-\epsilon)} R_x^{\eta\epsilon} D_x^{-\eta}} + 1 - q$, (b) follows from multi-nominal series and the moment generation function of $r(\Phi_{\mathrm{BS}}, \Phi_u)$ with $C_1 : n_1, n_2, \cdots, n_M \geq 0$ and $C_2 : n_1 + n_2 + \cdots + n_M = b$. We notice that R, R_x and D_x are random variables. Let $T_1 = \mathbb{E}\left[\prod_{x\in\Phi_{\mathrm{I}}} \prod_{m=1}^{M} f(\theta_m)^{n_m}\right]$, we have

$$T_1 = \mathbb{E}_{R,R_x,D_x}\left[\prod_{x\in\Phi_{\mathrm{I}}}\prod_{m=1}^{M}\left(1 - \frac{q\theta_m}{\theta_m + R^{\eta(\epsilon-1)} D_x^{\eta} R_x^{-\eta\epsilon}}\right)^{n_m}\right]. \quad (32)$$

According to the distribution of R_x in (4), we furter have

$$T_1 = \mathbb{E}_{R,D_x}\left[\prod_{x\in\Phi_{\mathrm{I}}} f_{R_x}(x, D_x) \prod_{m=1}^{M}\left(1 - \frac{q\theta_m}{\theta_m + R^{\eta(\epsilon-1)} D_x^{\eta} x^{-\eta\epsilon}}\right)^{n_m}\right], \quad (33)$$

where $f_{R_x}(x, D_x) = \frac{2B_1\pi\lambda x e^{-B_1\lambda\pi x^2}}{1-e^{-B_1\lambda\pi D_x^2}}$. Further, following from the probability generating functional (PGFL) of PPP, we have

$$T_1 = \mathbb{E}_R\left[\exp\left(-2\pi\int_0^{\infty}\left(1 - \int_0^{a} f_{R_x}(x,a) \times \prod_{m=1}^{M} \left(1 - \frac{q\theta_m}{\theta_m + R^{\eta(\epsilon-1)} a^{\eta} x^{-\eta\epsilon}}\right)^{n_m} \mathrm{d}x\right) a\lambda\left(1 - e^{-B_2\lambda\pi a^2}\right)\mathrm{d}a\right)\right]. \quad (34)$$

Nextly, we calculate the expected value of the random variable R and perform several simplifications as follows,

$$\begin{aligned}
&\mathbb{E}_R\left[\exp\left(-2\pi\int_0^{\infty}\left(1 - \int_0^{a} f_{R_x}(x,a)\prod_{m=1}^{M}\left(1 - \frac{q\theta_m}{\theta_m + R^{\eta(\epsilon-1)} a^{\eta} x^{-\eta\epsilon}}\right)^{n_m}\mathrm{d}x\right) a\lambda\left(1 - e^{-B_2\lambda\pi a^2}\right)\mathrm{d}a\right)\right] \\
&= \int_0^{\infty} 2B_1\lambda\pi r e^{-B_1\lambda\pi r^2} \exp\left(\int_0^{\infty} -2\pi a\lambda\left(1 - e^{-B_2\lambda\pi a^2}\right)\left(1 - \int_0^{a} f_{R_x}(x,a)\prod_{m=1}^{M}\left(1 - \frac{q\theta_m}{\theta_m + r^{\eta(\epsilon-1)} a^{\eta} x^{-\eta\epsilon}}\right)^{n_m}\mathrm{d}x\right)\mathrm{d}a\right)\mathrm{d}r \\
&\overset{(a)}{=} \int_0^{\infty} 2B_1\lambda\pi r e^{-B_1\lambda\pi r^2} \exp\left(\int_0^{\infty} -2\pi\lambda r^2 v\left(1 - e^{-B_2\lambda\pi v^2 r^2}\right)\left(1 - \int_0^{v} f_{R_x}(u,v)\prod_{m=1}^{M}\left(1 - \frac{q\theta_m}{\theta_m + v^{\eta} u^{-\eta\epsilon}}\right)^{n_m}\mathrm{d}u\right)\mathrm{d}v\right)\mathrm{d}r \\
&\overset{(b)}{=} \int_0^{\infty} e^{-z} \exp\left(\int_0^{\infty} -\frac{z}{B_1}\left(1 - e^{-\frac{B_2}{B_1} z v}\right)\left(1 - \int_0^{v}\frac{z e^{-zu}}{1-e^{-zv}}\prod_{m=1}^{M}\left(1 - \frac{q\theta_m}{\theta_m + v^{\frac{\eta}{2}} u^{-\frac{\eta\epsilon}{2}}}\right)^{n_m}\mathrm{d}u\right)\mathrm{d}v\right)\mathrm{d}z \\
&\overset{(c)}{=} \int_0^{\infty} \exp\left(-z\left(1 + \int_0^{\infty}\int_0^{x}\frac{\left(1 - e^{-\frac{B_2}{B_1} z x}\right) z e^{-zy}}{B_1\left(1 - e^{-zx}\right)}\left(1 - \prod_{m=1}^{M}\left(1 - \frac{q\theta_m}{\theta_m + x^{\frac{\eta}{2}} y^{-\frac{\eta\epsilon}{2}}}\right)^{n_m}\right)\right)\mathrm{d}y\mathrm{d}x\right)\mathrm{d}z,
\end{aligned} \quad (35)$$

where $f(x,z) = \int_0^x \frac{\left(1-e^{-\frac{B_2}{B_1} z x}\right) z e^{-zy} h(x,y)}{B_1\left(1-e^{-zx}\right)}\mathrm{d}y$ and $h(x,y) = \left(1 - \prod_{m=1}^{M}\left(1 - \frac{q\theta_m}{\theta_m + x^{\frac{\eta}{2}} y^{-\frac{\eta\epsilon}{2}}}\right)^{n_m}\right)$. (a) follows the distribution of R, $u = x/r$ and $v = a/r$, (b) is obtained by $v = v^2$, $u = u^2$ and $z = B_1\lambda\pi r^2$, (c) is derived from $x = v, y = u$ and $1 = \int_0^x \frac{z e^{-zy}}{1-e^{-zx}}$. The proof is complete.

References

[1] J. Navarro-Ortiz, P. Romero-Diaz, S. Sendra, P. Ameigeiras, J. J. Ramos-Munoz, and J. M. Lopez-Soler, "A survey on 5G usage scenarios and traffic models," *IEEE Commun. Surv. Tutor.*, vol. 22, no. 2, pp. 905–929, Feb. 2020.

[2] *5G; NR; Physical Channels and Modulation (3GPP TS 38.211 version 15.2.0 Release 15)*, ETSI Std. ETSI TS 138 211 V15.2.0, Jul. 2018.

[3] L. Zhang, J. Tan, Y.-C. Liang, G. Feng, and D. Niyato, "Deep reinforcement learning-based modulation and coding scheme selection in cognitive heterogeneous networks," *IEEE Trans. Wireless Commun.*, vol. 18, no. 6, pp. 3281–3294, Apr. 2019.

[4] Y. Kryukov, D. Pokamestov, A. Brovkin, A. Shinkevich, and G. Shalin, "MCS map for link-level simulation of two-user PD-NOMA system," *Proceedings on Engineering*, vol. 6, no. 1, pp. 151–160, 2024.

[5] X. Ye, Y. Yu, and L. Fu, "Deep reinforcement learning based link adaptation technique for LTE/NR systems," *IEEE Trans. Veh. Technol.*, vol. 72, no. 6, pp. 7364–7379, Jan. 2023.

[6] E. Bobrov, D. Kropotov, H. Lu, and D. Zaev, "Massive MIMO adaptive modulation and coding using online deep learning algorithm," *IEEE Commun. Lett.*, vol. 26, no. 4, pp. 818–822, Dec. 2022.

[7] Y. Hmamouche, M. Benjillali, S. Saoudi, H. Yanikomeroglu, and M. Di Renzo, "New trends in stochastic geometry for wireless networks: A tutorial and survey," *Proc. IEEE*, vol. 109, no. 7, pp. 1200–1252, Mar. 2021.

[8] P. D. Mankar, B. R. Sahu, G. Das, and S. S. Pathak, "Evaluation of blocking probability for downlink in Poisson networks," *IEEE Wireless Commun. Lett.*, vol. 4, no. 6, pp. 625–628, Sep. 2015.

[9] A. Papazafeiropoulos, P. Kourtessis, M. Di Renzo, S. Chatzinotas, and J. M. Senior, "Performance analysis of cell-free massive MIMO systems: A stochastic geometry approach," *IEEE Trans. Veh. Technol.*, vol. 69, no. 4, pp. 3523–3537, Jan. 2020.

[10] T. Wang, G. Chen, M.-A. Badiu, and J. P. Coon, "Performance analysis of RIS-assisted large-scale wireless networks using stochastic geometry," *IEEE Trans. Wireless Commun.*, vol. 22, no. 11, pp. 7438–7451, Mar. 2023.

[11] F. J. Martin-Vega, M. C. Aguayo-Torres, G. Gómez, and M. Di Renzo, "Interference-aware muting for the uplink of heterogeneous cellular networks: A stochastic geometry approach," in *Proc. IEEE Int. Conf. Commun. (ICC)*, Paris, France, Jul. 2017, pp. 1–6.

[12] Y. Wang, M. Haenggi, and Z. Tan, "The meta distribution of the SIR for cellular networks with power control," *IEEE Trans. Commun.*, vol. 66, no. 4, pp. 1745–1757, Dec. 2017.

[13] S. Wang and M. Di Renzo, "On the meta distribution in spatially correlated non-Poisson cellular networks," *EURASIP Journal on Wireless Communications and Networking*, vol. 2019, pp. 1–11, 2019.

[14] M. Haenggi, "User point processes in cellular networks," *IEEE Wireless Commun. Lett.*, vol. 6, no. 2, pp. 258–261, Feb. 2017.

[15] X. Lu, M. Salehi, M. Haenggi, E. Hossain, and H. Jiang, "Stochastic geometry analysis of spatial-temporal performance in wireless networks: A tutorial," *IEEE Commun. Surv. Tuts.*, vol. 23, no. 4, pp. 2753–2801, Aug. 2021.